Structural Engineering and Mechanics, *Vol. 72, No. 3 (2019) 329-338*
DOI: https://doi.org/10.12989/sem.2019.72.3.329

Modeling wave propagation in graphene sheets influenced by magnetic field via a refined trigonometric two-variable plate theory

R. Ebrahimi Fardshad*[1], Y. Mohammadi[1] and F. Ebrahimi*[2]

[1]*Department of Mechanical Engineering, Faculty of Industrial and Mechanical Engineering, Islamic Azad University, Qazvin Branch, Qazvin, Iran*
[2]*Department of Mechanical Engineering, Faculty of Engineering, Imam Khomeini International University, Qazvin, Iran*

(Received August 18, 2018, Revised April 19, 2019, Accepted June 4, 2019)

Abstract. In this paper, the magnetic field influence on the wave propagation characteristics of graphene nanosheets is examined within the frame work of a two-variable plate theory. The small-scale effect is taken into consideration based on the nonlocal strain gradient theory. For more accurate analysis of graphene sheets, the proposed theory contains two scale parameters related to the nonlocal and strain gradient effects. A derivation of the differential equation is conducted, employing extended principle of Hamilton and solved my means of analytical solution. A refined trigonometric two-variable plate theory is employed in Kinematic relations. The scattering relation of wave propagation in solid bodies which captures the relation of wave number and the resultant frequency is also investigated. According to the numerical results, it is revealed that the proposed modeling can provide accurate wave dispersion results of the graphene nanosheets as compared to some cases in the literature. It is shown that the wave dispersion characteristics of graphene sheets are influenced by magnetic field, elastic foundation and nonlocal parameters. Numerical results are presented to serve as benchmarks for future analyses of graphene nanosheets.

Keywords: refined-trigonometric two-variable plate theory; magnetic field effects; wave dispersion; graphene nanosheets; Nonlocal strain gradient theory (NSGT);

1. Introduction

Recent researches have revealed that Graphene exhibits exceptional electronic and mechanical properties due to its unique atomic structure. These phenomenal characteristics of Graphene can be exploited thoroughly in various nano-engineering applications such as sensors, actuators, energy harvesters, micro-electro mechanical systems (MEMS) etc. Due to its tremendous engineering applications, much of the focus is placed on the vibration and wave propagation analysis of graphene structures in nano-engineering. As a matter of fact, that the graphene sheets are sufficiently small (nano scale), it is very much necessary to consider the effects of length scale in order to apply classical models of elasticity. It cannot be denied that the mechanical responses of nanostructures are different in contrast to the macrostructures. Therefore, in the recent years, a severe tendency is observed in the research society to accurately assess the mechanical responses of nanostructures. In this regard, the size-dependent nonlocal continuum models and various theories are proved to be efficient and beneficial. For the first time, Eringen put forward the first nonlocal theory, called nonlocal elasticity theory (NET), to take into consideration the size-dependency of nanostructures (Eringen 1972, 1983). In his research, Eringen pointed that stress state at each desired point in a solid body is affected by two main variants; first, the strain in that point, and second, strain in all other neighboring points. This theory is broadly applied in many papers dealing with the mechanical behavior of nano-structures.

Many pioneers have exploited the benefit of NET and highlighted its significance for wave propagation analysis (Wang and Varadan 2007, Wang *et al.* 2010, Narendar and Gopalakrishnan 2012a, b), free vibration analysis (Malekzadeh *et al.* 2011, Eltaher *et al.* 2013, Ebrahimi and Salari 2015b) and bending and buckling analysis (Aydogdu 2009) of various nano structures. Ebrahimi and his co-workers utilized the NET to investigate the mechanical responses of size-dependent beams and plates subjected to various external load (Ebrahimi and Salari 2015, Ebrahimi *et al.* 2016b, 2017, Ebrahimi and Dabbagh 2017b,c, Ebrahimi and Barati 2017). Even though the enormous use of the NET for investigating the mechanical responses of tiny structures has been witnessed, there are some drawbacks associated with this theory based on the experiments (Fleck and Hutchinson 1993, Lam *et al.* 2003). Meanwhile, Lam *et al.* (2003) showed the crucial role of elastic strain gradient in the size-dependent responses of small structures. Further, NET considers only the stiffness softening effect. Also, NET fails to incorporate stiffness-hardening effect by introducing the length scale parameter. Lately, Lim *et al.* (2015) presented a new nonlocal continuum theory, named nonlocal strain gradient theory (NSGT), to account for the small scale influences precisely.

*Corresponding author, Professor
E-mail: raminfardshad@gmail.com

ISSN: 1225-4568 (Print), 1598-6217 (Online)

In this theory, both of the previous behaviors discussed by Eringen (1972, 1983) and Lam *et al.* (2003) are covered. In addition, the stress field of NSGT accounts for not only the nonlocal stress field but also the strain gradient stress field. Also, Lim *et al.* (2015) justified the credibility of this theory by analyzing the wave dispersion responses of CNTs. This paved way for further works as many researchers attempted to use this theory for studying the mechanical response of nanostructures. The solution to evaluate the buckling problem of nanobeams and nano plates through NSGT was proposed by Li and Hu (2015) and Farajpour *et al.* (2016), respectively. The wave dispersion properties of nano-beams and –plates are investigated in detail in the framework of the NSGT by Ebrahimi and his co-workers (Ebrahimi *et al.* 2016a, Ebrahimi and Dabbagh 2017a). Most recently, Ebrahimi and Barati (2018) developed a NSGT to analyze the vibration problem of an axially functionally graded nanobeam. Khelifa *et al*. (2018) explored the buckling response with stretching effect of carbon nanotube-reinforced composite beams resting on elastic foundation. In another work, Bending and free vibration analysis of FG plates was investigated by Bellifa *et al*. (2016) using a simple shear deformation theory and the concept the neutral surface position. Ould Larbi (2018) presented an analytical solution for free vibration of functionally graded beam using a simple first-order shear deformation theory while Zouatnia *et al*. (2017) presented an analytical solution for bending and vibration responses of functionally graded beams with porosities. Recently, Hadji *et al*. (2018) employed a new quasi-3D higher shear deformation theory for vibration of functionally graded carbon nanotube-reinforced composite beams resting on elastic foundation. A new higher order and sinusoidal shear deformation model was introduced by Hadji *et al*. (2017a) for functionally graded beams and plates.

Parallelly, it was evident from the researches that a large variety of carbon based structures such as CNTs, carbon nanocones and nanorings can be achieved by generating some controlled distortions in single-layered graphene sheets (SLGSs) (Ghorbanpour Arani and Jalaei 2016). In addition, graphene sheets encompass some superiorities compared with other small size structures made of many various types of materials like higher elastic potential (Lee *et al.* 2008) and larger thermal conductivity (Seol *et al.* 2010). Owing to the beneficial properties of SLGS, it becomes crucial to thoroughly explore and understand the mechanical responses of SLGS structures under the influence of various external loadings (Murmu and Pradhan 2009, Pradhan and Murmu 2010, Pradhan and Kumar 2011, Rouhi and Ansari 2012). Also, the effect of external magnetic field on the vibration characteristics of SLGS was studied by Murmu *et al.* (2013) and Ghorbanpour Arani *et al.* (2016). Meanwhile, Zenkour (2016) surveyed the transient vibration problem of a SLGS rested on a viscoelastic foundation. Influence of initial shear stress is regarded by Ebrahimi and Shafiei (2017) analyzing vibrational characteristics of SLGSs rested on Winkler-Pasternak foundation.

Literature review reveals a surge inclination in the research society investigating the vibration and buckling analysis of SLGSs, whereas, the wave propagation answers are available in scarce. However, the prominent applications of wave propagation-based methods in many industrial applications satisfy everybody to pay more attention to the wave propagation analysis of mechanical elements. Lately, more time and energy effort are allocated to the investigation of wave propagation responses of SLGSs. For example, size-dependent mechanical properties of propagating waves in graphene sheets are exactly studied by Arash *et al.* (2012) by the means of the nonlocal elasticity. Also, Liu and Yang (2012) employed a nonlocal model to investigate the wave propagation problem of an embedded isotropic graphene sheet. Hadji *et al*. (2017b) presented the wave propagation in functionally graded beams using various higher-order shear deformation beams theories. Most recently, Xiao *et al.* (2017) presented a nonlocal strain gradient based theory to examine wave propagation behaviors of viscoelastic monolayer graphene sheets.

From the exhaustive literature survey, it is clear that wave propagation behavior of NSG based SLGSs with respect to the effects of the induced Lorentz force has not been studied hitherto. In this regard, the present work makes the first attempt. The graphene sheet is modeled via a refined higher-order two-variable plate theory. Also, NSGT is utilized in order to describe the small-scale effects in detail by capturing both stiffness-softening and –hardening impacts. Moreover, SLGS is assumed to be rested on a two-parameter elastic medium. Maxwell's equation is satisfied in the x axis and the generated Lorentz force is calculated. In addition, the principle of virtual work is employed to derive the Euler-Lagrange equations. Afterwards, the obtained differential equations are incorporated with those on the NSGT to develop the nonlocal governing equations of SLGSs. In the framework of an analytical exponential solution procedure, the wave frequency, phase velocity and escape frequencies are achieved.

2. Theory and formulation

2.1 Kinematic relations

Present part is devoted to describing the kinematic behaviors of graphene sheets. The schematic of an embedded SLGS can be seen in Fig. 1. In order to capture shear deformation effects, a refined trigonometric two-variable plate theory is utilized. Thus, the displacement fields can be written as:

$$U\left(x,y,z,t\right)=-z\frac{\partial w_b}{\partial x}-f\left(z\right)\frac{\partial w_s}{\partial x} \tag{1}$$

$$V\left(x,y,z,t\right)=-z\frac{\partial w_b}{\partial y}-f\left(z\right)\frac{\partial w_s}{\partial y} \tag{2}$$

$$W\left(x,y,z,t\right)=w_b\left(x,y,t\right)+w_s\left(x,y,t\right) \tag{3}$$

where w_b and w_s are bending and shear deflections in the thickness direction, respectively. Also, $f(z)$ is a shape

function that estimates shear stress and shear strain. In the present theory, a trigonometric function is used as follows

$$f(z)=z-\frac{h}{\pi}\sin\left(\frac{\pi z}{h}\right) \tag{4}$$

in above equation, h is plate's thickness. Now, the nonzero strains can be stated as follows

$$\begin{Bmatrix}\varepsilon_x\\ \varepsilon_y\\ \gamma_{xy}\end{Bmatrix}=z\begin{Bmatrix}-\dfrac{\partial^2 w_b}{\partial x^2}\\ -\dfrac{\partial^2 w_b}{\partial y^2}\\ -2\dfrac{\partial^2 w_b}{\partial x\partial y}\end{Bmatrix}+ f(z)\begin{Bmatrix}-\dfrac{\partial^2 w_s}{\partial x^2}\\ -\dfrac{\partial^2 w_s}{\partial y^2}\\ -2\dfrac{\partial^2 w_s}{\partial x\partial y}\end{Bmatrix},\ \begin{Bmatrix}\gamma_{yz}\\ \gamma_{xz}\end{Bmatrix}=g(z)\begin{Bmatrix}\dfrac{\partial w_s}{\partial y}\\ \dfrac{\partial w_s}{\partial x}\end{Bmatrix} \tag{5}$$

in Eq. (5), $g(z)$ can be stated as

$$g(z)=1-\frac{df(z)}{dz} \tag{6}$$

Besides, the Hamilton's principle can be defined as

$$\int_0^t \delta(U-T+V)\,dt=0 \tag{7}$$

in which U is strain energy, T is kinetic energy and V is work done by external loads. The variation of strain energy can be calculated as

$$\delta U=\int_V \sigma_{ij}\delta\varepsilon_{ij}dV=\int_V\left(\sigma_x\delta\varepsilon_x+\sigma_y\delta\varepsilon_y+\sigma_{xy}\delta\gamma_{xy}+\sigma_{yz}\delta\gamma_{yz}+\sigma_{xz}\delta\gamma_{xz}\right)dV \tag{8}$$

Substituting Eq. (5) in Eq. (8) reveals

$$\delta U=\int_0^a\int_0^b\begin{pmatrix}-M_x^b\dfrac{\partial^2\delta w_b}{\partial x^2}-M_x^s\dfrac{\partial^2\delta w_s}{\partial x^2}-M_y^b\dfrac{\partial^2\delta w_b}{\partial y^2}-M_y^s\dfrac{\partial^2\delta w_s}{\partial y^2}-\\ 2M_{xy}^b\dfrac{\partial^2\delta w_b}{\partial x\partial y}-2M_{xy}^s\dfrac{\partial^2\delta w_s}{\partial x\partial y}+Q_{xz}\dfrac{\partial\delta w_s}{\partial x}+Q_{yz}\dfrac{\partial\delta w_s}{\partial y}\end{pmatrix}dydx \tag{9}$$

in Eq. (9) the unknown parameters can be defined in the following form

$$\begin{aligned}\left(M_i^b,M_i^s\right)&=\int_{-h/2}^{h/2}\left(z,f\right)\sigma_i dz,\ i=(x,y,xy)\\ Q_i&=\int_{-h/2}^{h/2} g\sigma_i dz,\ i=(xz,yz)\end{aligned} \tag{10}$$

Furthermore, work done by external forces can be divided in two parts; one part is generated due to the elastic medium and another one is the external work of Lorentz force induced by the magnetic field. Indeed, the SLGS is presumed to be subjected to a longitudinal steady magnetic field with the intensity of H_0. Hence, the exerted body force produced by this field can be formulated as follows

$$f_{Lz}=\eta\underbrace{\left(\underbrace{\nabla\times\left(\nabla\times\left(u\times H_0\right)\right)}_{h}\right)}_{J}\times H_0 \tag{11}$$

in which η, ∇, h and J are the magnetic permeability of SLGS, gradient operator, small disturbance of applied magnetic field and current density vector, respectively. Here, the magnetic field can be expressed as follows

$$H_0=H_x\delta_x\hat{i} \tag{12}$$

where, δ is the Kronecker delta tensor. Inserting Eqs. (1) to (3) in Eq. (11), the applied Lorentz forces per unit volume can be written as

$$f_{Lz}=\eta H_x{}^2\frac{\partial^2\left(w_b+w_s\right)}{\partial x^2} \tag{13}$$

Furthermore, the resultant Lorentz's forces can be written in the following form

$$F_{Lz}=\int_{-h/2}^{h/2} f_{Lz}dz=\eta h H_x{}^2\frac{\partial^2\left(w_b+w_s\right)}{\partial x^2} \tag{14}$$

Thus, the work done by external forces can be expressed as

$$\delta V=\int_0^a\int_0^b\begin{pmatrix}-k_w\delta(w_b+w_s)+k_p\begin{pmatrix}+\dfrac{\partial(w_b+w_s)}{\partial x}\dfrac{\partial\delta(w_b+w_s)}{\partial x}\\ +\dfrac{\partial(w_b+w_s)}{\partial y}\dfrac{\partial\delta(w_b+w_s)}{\partial y}\end{pmatrix}\\ -\eta h H_x{}^2\dfrac{\partial^2\left(w_b+w_s\right)}{\partial x^2}\end{pmatrix}dydx \tag{15}$$

where k_w and k_p are Winkler and Pasternak coefficients. The variation of the kinetic energy should be written as

$$\delta K=\int_0^a\int_0^b\begin{pmatrix}I_0\left(\dfrac{\partial(w_b+w_s)}{\partial t}\dfrac{\partial\delta(w_b+w_s)}{\partial t}\right)+I_2\left(\dfrac{\partial w_b}{\partial x\partial t}\dfrac{\partial\delta w_b}{\partial x\partial t}+\dfrac{\partial w_b}{\partial y\partial t}\dfrac{\partial\delta w_b}{\partial y\partial t}\right)\\ +K_2\left(\dfrac{\partial w_s}{\partial x\partial t}\dfrac{\partial\delta w_s}{\partial x\partial t}+\dfrac{\partial w_s}{\partial y\partial t}\dfrac{\partial\delta w_s}{\partial y\partial t}\right)+\\ J_2\left(\dfrac{\partial w_b}{\partial x\partial t}\dfrac{\partial\delta w_s}{\partial x\partial t}+\dfrac{\partial w_s}{\partial x\partial t}\dfrac{\partial\delta w_b}{\partial x\partial t}+\dfrac{\partial w_b}{\partial y\partial t}\dfrac{\partial\delta w_s}{\partial y\partial t}+\dfrac{\partial w_s}{\partial y\partial t}\dfrac{\partial\delta w_b}{\partial y\partial t}\right)\end{pmatrix}dydx \tag{16}$$

in which

$$\left(I_0,I_2,J_2,K_2\right)=\int_{-h/2}^{h/2}\left(1,z^2,zf,f^2\right)\rho dz \tag{17}$$

Inserting Eqs. (9), (15) and (16) in Eq. (7) and setting the coefficients of δw_b and δw_s to zero, the Euler-Lagrange

equations of GSs can be rewritten as

$$\begin{aligned}&\frac{\partial^2 M_x^b}{\partial x^2}+2\frac{\partial^2 M_{xy}^b}{\partial x\partial y}+\frac{\partial^2 M_y^b}{\partial y^2}\\&+k_p\nabla^2(w_b+w_s)-k_w(w_b+w_s)=\\&I_0\frac{\partial^2(w_b+w_s)}{\partial t^2}-I_2\nabla^2\left(\frac{\partial^2 w_b}{\partial t^2}\right)\\&-J_2\nabla^2\left(\frac{\partial^2 w_s}{\partial t^2}\right)-\eta h H_x{}^2\frac{\partial^2(w_b+w_s)}{\partial x^2}\end{aligned} \tag{18}$$

$$\begin{aligned}&\frac{\partial^2 M_x^s}{\partial x^2}+2\frac{\partial^2 M_{xy}^s}{\partial x\partial y}+\frac{\partial^2 M_y^s}{\partial y^2}+\frac{\partial Q_{xz}}{\partial x}+\frac{\partial Q_{yz}}{\partial y}\\&+k_p\nabla^2(w_b+w_s)-k_w(w_b+w_s)\\&=I_0\frac{\partial^2(w_b+w_s)}{\partial t^2}-J_2\nabla^2\left(\frac{\partial^2 w_b}{\partial t^2}\right)\\&-K_2\nabla^2\left(\frac{\partial^2 w_s}{\partial t^2}\right)-\eta h H_x{}^2\frac{\partial^2(w_b+w_s)}{\partial x^2}\end{aligned} \tag{19}$$

2.2 The nonlocal strain gradient theory

According to the nonlocal strain gradient theory, the stress field takes into consider the effects of nonlocal elastic stress field besides strain gradient stress field. So, the theory can be expressed as follows for elastic solids

$$\sigma_{ij}=\sigma_{ij}^{(0)}-\frac{d\sigma_{ij}^{(1)}}{dx} \tag{20}$$

in above equation, the stresses $\sigma_{xx}^{(0)}$ (classical stress) and $\sigma_{xx}^{(1)}$ (higher-order stress) are corresponding to strain ε_{xx} and strain gradient $\varepsilon_{xx,x}$, respectively as follows

$$\begin{cases}\sigma_{ij}^{(0)}=\int_0^L C_{ijkl}\alpha_0(x,x',e_0a)\varepsilon'_{kl}(x')dx'\\ \sigma_{ij}^{(1)}=l^2\int_0^L C_{ijkl}\alpha_1(x,x',e_1a)\varepsilon'_{kl,x}(x')dx'\end{cases} \tag{21}$$

in which C_{ijkl} is the elastic coefficient; e_0a and e_1a are introduced to account for the nonlocality effects. Also, l captures the strain gradient effects. Once the nonlocal kernel functions $\alpha_0(x,x',e_0a)$ and $\alpha_1(x,x',e_1a)$ satisfy the developed conditions, the constitutive relation of nonlocal strain gradient theory can be expressed as below

$$\begin{aligned}&\left(1-(e_1a)^2\nabla^2\right)\left(1-(e_0a)^2\nabla^2\right)\sigma_{ij}\\&=C_{ijkl}\left(1-(e_1a)^2\nabla^2\right)\varepsilon_{kl}-C_{ijkl}\,l^2\left(1-(e_0a)^2\nabla^2\right)\nabla^2\varepsilon_{kl}\end{aligned} \tag{22}$$

in which ∇^2 denotes the Laplacian operator. Considering $e_0=e_1=e$, the general constitutive relation in Eq. (22) becomes

$$\left(1-(ea)^2\nabla^2\right)\sigma_{ij}=C_{ijkl}\left(1-l^2\nabla^2\right)\varepsilon_{kl} \tag{23}$$

Finally, the simplified constitutive relation can be written as follows

$$\begin{aligned}&\left(1-\mu^2\nabla^2\right)\begin{Bmatrix}\sigma_x\\ \sigma_y\\ \sigma_{xy}\\ \sigma_{yz}\\ \sigma_{xz}\end{Bmatrix}\\&=\left(1-\lambda^2\nabla^2\right)\begin{pmatrix}Q_{11}&Q_{12}&0&0&0\\ Q_{12}&Q_{22}&0&0&0\\ 0&0&Q_{66}&0&0\\ 0&0&0&Q_{44}&0\\ 0&0&0&0&Q_{55}\end{pmatrix}\begin{Bmatrix}\varepsilon_x\\ \varepsilon_y\\ \gamma_{xy}\\ \gamma_{yz}\\ \gamma_{xz}\end{Bmatrix}\end{aligned} \tag{24}$$

in above equation

$$\begin{aligned}&Q_{11}=Q_{22}=\frac{E}{1-\nu^2},\\&Q_{12}=\nu Q_{11},\\&Q_{44}=Q_{55}=Q_{66}=\frac{E}{2(1+\nu)}\end{aligned} \tag{25}$$

where $\mu=e_0a$ and $\lambda=l$. Substituting Eq. (10) in Eq. (24) gives

$$\begin{aligned}&\left(1-\mu^2\nabla^2\right)\begin{Bmatrix}M_x^b\\ M_y^b\\ M_{xy}^b\end{Bmatrix}\\&=\left(1-\lambda^2\nabla^2\right)\left(\begin{pmatrix}D_{11}&D_{12}&0\\ D_{12}&D_{22}&0\\ 0&0&D_{66}\end{pmatrix}\begin{Bmatrix}-\frac{\partial^2 w_b}{\partial x^2}\\ -\frac{\partial^2 w_b}{\partial y^2}\\ -2\frac{\partial^2 w_b}{\partial x\partial y}\end{Bmatrix}+\begin{pmatrix}D_{11}^s&D_{12}^s&0\\ D_{12}^s&D_{22}^s&0\\ 0&0&D_{66}^s\end{pmatrix}\begin{Bmatrix}-\frac{\partial^2 w_s}{\partial x^2}\\ -\frac{\partial^2 w_s}{\partial y^2}\\ -2\frac{\partial^2 w_s}{\partial x\partial y}\end{Bmatrix}\right)\end{aligned} \tag{26}$$

$$\begin{aligned}&\left(1-\mu^2\nabla^2\right)\begin{Bmatrix}M_x^s\\ M_y^s\\ M_{xy}^s\end{Bmatrix}\\&=\left(1-\lambda^2\nabla^2\right)\left(\begin{pmatrix}D_{11}^s&D_{12}^s&0\\ D_{12}^s&D_{22}^s&0\\ 0&0&D_{66}^s\end{pmatrix}\begin{Bmatrix}-\frac{\partial^2 w_b}{\partial x^2}\\ -\frac{\partial^2 w_b}{\partial y^2}\\ -2\frac{\partial^2 w_b}{\partial x\partial y}\end{Bmatrix}+\begin{pmatrix}H_{11}^s&H_{12}^s&0\\ H_{12}^s&H_{22}^s&0\\ 0&0&H_{66}^s\end{pmatrix}\begin{Bmatrix}-\frac{\partial^2 w_s}{\partial x^2}\\ -\frac{\partial^2 w_s}{\partial y^2}\\ -2\frac{\partial^2 w_s}{\partial x\partial y}\end{Bmatrix}\right)\end{aligned} \tag{27}$$

$$\left(1-\mu^2\nabla^2\right)\begin{Bmatrix}Q_x\\ Q_y\end{Bmatrix}=\left(1-\lambda^2\nabla^2\right)\left(\begin{pmatrix}A_{44}^s&0\\ 0&A_{55}^s\end{pmatrix}\begin{Bmatrix}\frac{\partial w_s}{\partial x}\\ \frac{\partial w_s}{\partial y}\end{Bmatrix}\right) \tag{28}$$

in Eqs. (26) to (28), the cross-sectional rigidities can be

formulated as follows

$$\begin{pmatrix} D_{11} & D_{11}^{s} & H_{11}^{s} \\ D_{12} & D_{12}^{s} & H_{12}^{s} \\ D_{66} & D_{66}^{s} & H_{66}^{s} \end{pmatrix} = \int_{-h/2}^{h/2} Q_{11}\begin{pmatrix} z^2 & zf & f^2 \end{pmatrix}\begin{Bmatrix} 1 \\ \nu \\ \dfrac{1-\nu}{2} \end{Bmatrix} dz \tag{29}$$

$$A_{44}^{s} = A_{55}^{s} = \int_{-h/2}^{h/2} g^2 \frac{E}{2(1+\nu)} dz \tag{30}$$

By substituting Eqs. (26) to (28) in Eqs. (18) and (19), the nonlocal governing equations of SLGSs can be directly derived in terms of displacements as follows

$$\begin{pmatrix} (1-\lambda^2\nabla^2)\begin{pmatrix} -D_{11}\dfrac{\partial^4 w_b}{\partial x^4} - 2(D_{12}+2D_{66})\dfrac{\partial^4 w_b}{\partial x^2\partial y^2} - D_{22}\dfrac{\partial^4 w_b}{\partial y^4} \\ -D_{11}^{s}\dfrac{\partial^4 w_s}{\partial x^4} - 2(D_{12}^{s}+2D_{66}^{s})\dfrac{\partial^4 w_s}{\partial x^2\partial y^2} - D_{22}^{s}\dfrac{\partial^4 w_s}{\partial y^4} \end{pmatrix} + (1-\mu^2\nabla^2) \\ \begin{pmatrix} -I_0\dfrac{\partial^2(w_b+w_s)}{\partial t^2} + I_2\left(\dfrac{\partial^4 w_b}{\partial x^2\partial t^2} + \dfrac{\partial^4 w_b}{\partial y^2\partial t^2}\right) + J_2\left(\dfrac{\partial^4 w_s}{\partial x^2\partial t^2} + \dfrac{\partial^4 w_s}{\partial y^2\partial t^2}\right) \\ +k_p\left(\dfrac{\partial^2(w_b+w_s)}{\partial x^2} + \dfrac{\partial^2(w_b+w_s)}{\partial y^2}\right) - k_w(w_b+w_s) + F_{Lz} \end{pmatrix} \end{pmatrix} = 0 \tag{31}$$

$$\begin{pmatrix} (1-\eta^2\nabla^2)\begin{pmatrix} -D_{11}^{s}\dfrac{\partial^4 w_b}{\partial x^4} - 2(D_{12}^{s}+2D_{66}^{s})\dfrac{\partial^4 w_b}{\partial x^2\partial y^2} - D_{22}^{s}\dfrac{\partial^4 w_b}{\partial y^4} \\ -H_{11}^{s}\dfrac{\partial^4 w_s}{\partial x^4} - 2(H_{12}^{s}+2H_{66}^{s})\dfrac{\partial^4 w_s}{\partial x^2\partial y^2} - H_{22}^{s}\dfrac{\partial^4 w_s}{\partial y^4} \\ +A_{44}^{s}\dfrac{\partial^2 w_s}{\partial x^2} + A_{55}^{s}\dfrac{\partial^2 w_s}{\partial y^2} \end{pmatrix} + (1-\mu^2\nabla^2) \\ \begin{pmatrix} -I_0\dfrac{\partial^2(w_b+w_s)}{\partial t^2} + J_2\left(\dfrac{\partial^4 w_b}{\partial x^2\partial t^2} + \dfrac{\partial^4 w_b}{\partial y^2\partial t^2}\right) + K_2\left(\dfrac{\partial^4 w_s}{\partial x^2\partial t^2} + \dfrac{\partial^4 w_s}{\partial y^2\partial t^2}\right) \\ +k_p\left(\dfrac{\partial^2(w_b+w_s)}{\partial x^2} + \dfrac{\partial^2(w_b+w_s)}{\partial y^2}\right) - k_w(w_b+w_s) + F_{Lz} \end{pmatrix} \end{pmatrix} = 0 \tag{32}$$

3. Analytical solution

In this part, the nonlocal governing equations derived in previous section are going to be solved analytically. The displacement fields are assumed to be exponential and can be defined as follows

$$\begin{Bmatrix} w_b(x,y,t) \\ w_s(x,y,t) \end{Bmatrix} = \begin{Bmatrix} W_b \exp\left[i(\beta_1 x + \beta_2 y - \omega t)\right] \\ W_s \exp\left[i(\beta_1 x + \beta_2 y - \omega t)\right] \end{Bmatrix} \tag{33}$$

where W_b and W_s are the unknown coefficients; β_1 and β_2 are the wave numbers of wave propagation along x and y directions respectively, and finally ω is wave's angular frequency. Now, substituting Eq. (33) to Eqs. (31) and (32) results

$$\left(\left[K\right]_{2\times 2} - \omega^2\left[M\right]_{2\times 2}\right)\{\Delta\} = \{0\} \tag{34}$$

The unknown parameters of Eq. (34) can be noted as follows

$$\{\Delta\} = \{W_b, W_s\}^T \tag{35}$$

In order to attaining wave's angular frequency, the determinant of the left hand side of Eq. (34) should be set to zero

$$\left|\left[K\right]_{2\times 2} - \omega^2\left[M\right]_{2\times 2}\right| = 0 \tag{36}$$

In above equation by setting $\beta_1 = \beta_2 = \beta$ and solving the obtained equation for ω, the wave's angular frequency of embedded SLGSs can be calculated. If the angular frequency is divided by wave number, the phase velocity can be obtained as below

$$c_p = \frac{\omega}{\beta} \tag{37}$$

Also, the escape frequency of graphene sheet can be derived by tending wave number to infinity

$$f_{esc} = \lim_{\beta\to\infty}\frac{\omega}{2\pi} \tag{1}$$

4. Numerical results and discussion

Herein, the wave propagation responses of SLGSs are compared once various parameters are supposed to be changed. The mechanical material properties of graphene sheets are: E=1 *TPa*, ν=0.19, ρ=2300 kg/m^3. Also, the thickness is presumed to be$h$=0.34 *nm*. In the following diagrams wave frequencies are calculated by dividing wave's angular frequency to 2π. Moreover, the validity of reported results is proven setting a comparison between results of present research with those of antecedent works.Fig. 2 is allocated to show the effects of both nonlocal and length scale parameters by plotting the variations of wave frequency versus wave number for different values of these parameters. Revealed from the diagram, nonlocal parameter is able to decrease the wave frequency once it is increased. Indeed, this effect which is named the stiffness-softening effect results in lowering wave frequency in wave numbers higher than $\beta = 3\times10^9$. In return, length scale parameter affects wave frequency in a

Table 1 Comparison of frequency of FG nanoplates for various nonlocal parameter (p=5)

μ	a/h=10		a/h=20	
	Natarajan *et al.* (2012)	present	Natarajan *et al.* (2012)	present
0	0.0441	0.043803	0.0113	0.011255
1	0.0403	0.040051	0.0103	0.010288
2	0.0374	0.037123	0.0096	0.009534
4	0.033	0.032791	0.0085	0.008418

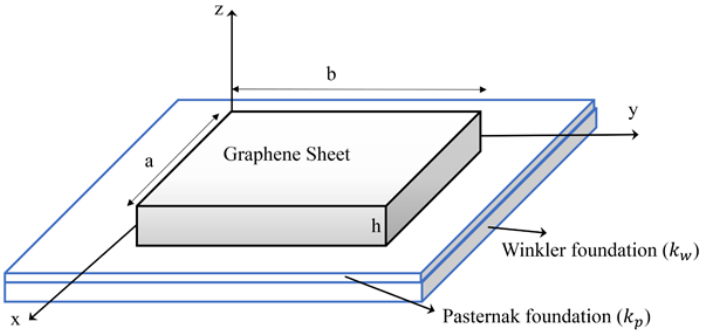

Fig. 1 Geometry of a single-layered graphene sheet rested on Winkler-Pasternak foundation.

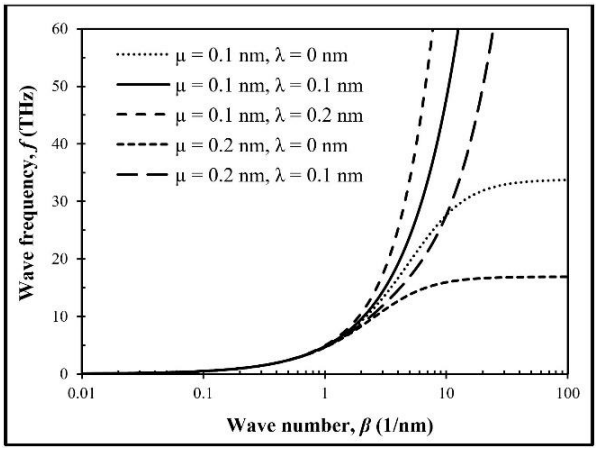

Fig. 2 Variation of wave frequency versus wave number for different nonlocal and length scale parameters (k_w= k_p =0, H_x=0)

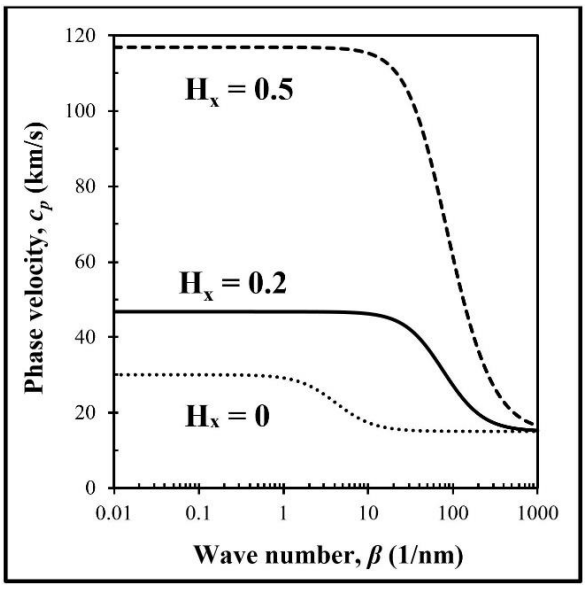

(a) λ<μ

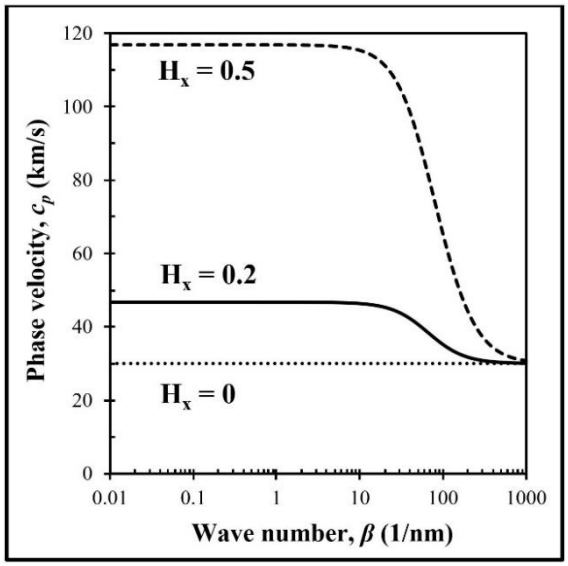

(b) λ=μ

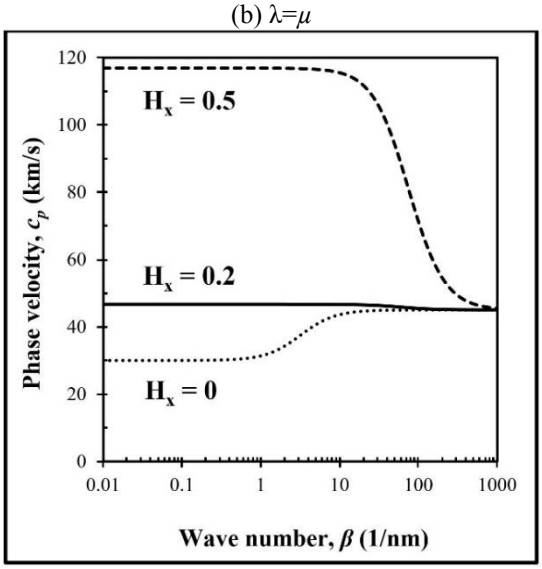

(c) λ>μ

Fig. 3 Variation of phase velocity versus wave number for various values of magnetic field intensity at (a) λ<μ, (b) λ=μ and (c) λ>μ (k_w = k_p = 0).

completely different way. Actually, a raise in the amount of wave frequency can be observed once greater length scale parameters are utilized. This increasing influence is named stiffness-hardening influence which has enough potential to strengthen the wave frequency values enormously.

Moreover, influence of magnetic field intensity is shown in Fig. 3. In this figure, variation of phase velocity versus

wave number is plotted for three main conditions ($\lambda<\mu$, $\lambda=\mu$ and $\lambda>\mu$) once magnetic field intensity is assumed to be changed. The main similarity between these three major situations is the increasing influence of magnetic field intensity on the phase velocity of graphene sheets. As a matter of fact, phase velocity can be aggrandized by applying higher amounts of magnetic field intensity. In the case of $\lambda<\mu$, phase velocity decreases continuously in each amount of magnetic field intensity. Moreover, whenever an equal amount is devoted to nonlocal and length scale parameters ($\lambda=\mu$), phase velocity has a constant value in all wave numbers once magnetic field intensity is set to zero; however, this variant experiences a decreasing trend in nonzero values of magnetic field intensity. Besides, whenever $\lambda>\mu$, phase velocity remains constant at first and then increases gradually once magnetic field intensity is set to zero.

In addition, Fig. 4 is depicted in order to magnify the influences of Winkler coefficient on the phase velocity of SLGSs for three major conditions ($\lambda<\mu$, $\lambda=\mu$ and $\lambda>\mu$). It is clear that Winkler coefficient affects phase velocity amounts once wave number is assumed to be smaller than $\beta = 0.04\times10^9$. Obviously, this parameter is powerful enough to motivate phase velocity values in the mentioned range of wave numbers. On the other hand, it is of significance to advert that phase velocity's behavior is a bit different in higher wave numbers once nonlocal and length scale parameters are supposed to obtain various amounts compared to each other. Precisely, phase velocity experiences a decreasing, unchangeable and increasing trend in the high wave numbers in the cases of $\lambda<\mu$, $\lambda=\mu$ and $\lambda>\mu$, respectively.

Now, it is turn to highlight the effects of nonlinear foundation parameter on the phase velocity of SLGSs for the same major conditions ($\lambda<\mu$, $\lambda=\mu$ and $\lambda>\mu$). Based on the Fig. 5, it shall be regarded that effects of Pasternak coefficient can be well observed in a wide range of wave numbers. Clearly, higher phase velocity amounts are achieved if greater Pasternak coefficients are employed. Moreover, it is clear to everybody that size-dependent behavior of SLGSs is happened in this diagram in the same form as occurred in the previous figure. In other words, once Pasternak coefficient is set to zero (k_p=0), wave responses of SLGSs in high wave numbers are hugely influenced by the ratio of nonlocal to length scale parameters. It is worth remarking that phase velocity shows a similar response in each of the three main cases once Pasternak parameter is obtained a nonzero value ($k_p\neq0$). In fact, in this condition ($k_p\neq0$), phase velocity achieves a same amount in the beginning and then starts a continuous decrease to its final value. Finally, coupled influences of nonlocal and length scale parameters are covered by plotting the variation of escape frequency versus nonlocal parameter for various length scale parameters in Fig. 6. In this diagram, it is avoided to use numerical nonzero amounts for other participant parameters because these parameters are not able to affect escape frequency ($\beta\to\infty$). Herein, previous results are confirmed again. Actually, it is clear that escape frequency goes through a gradual decreasing trend as nonlocality increases. However, escape frequency can be amplified by applying higher amounts for length scale parameters.

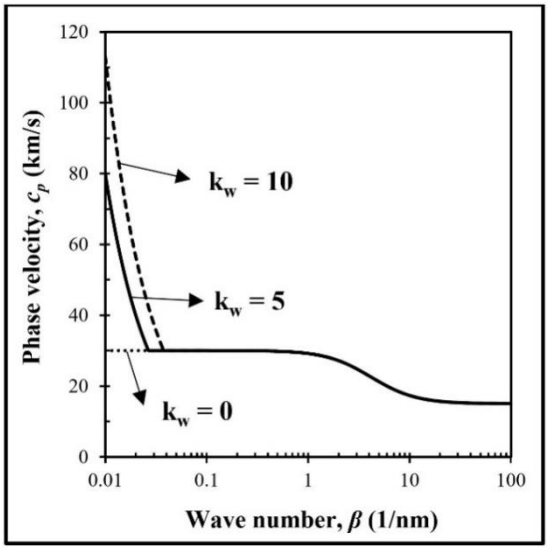

(a) $\lambda<\mu$

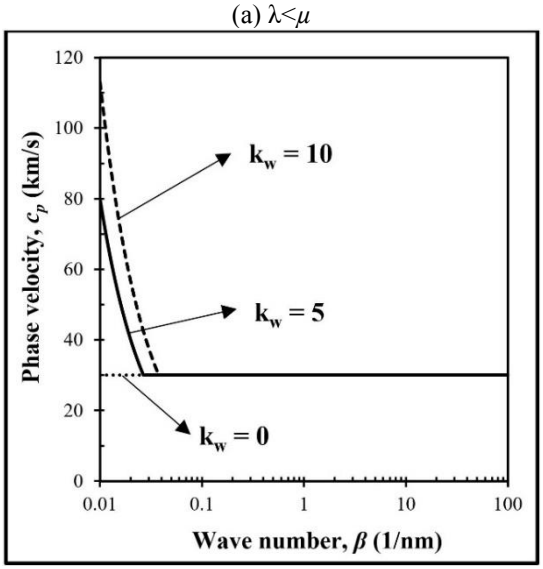

(b) $\lambda=\mu$

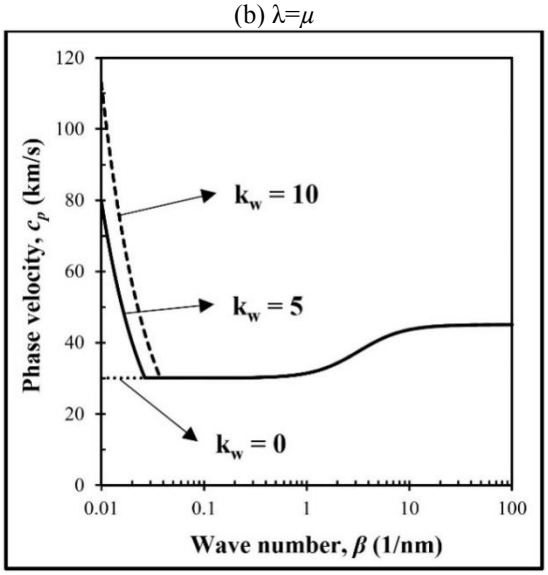

(c) $\lambda>\mu$

Fig. 4 4 Variation of phase velocity versus wave number for various values of Winkler coefficient at (a) $\lambda<\mu$, (b) $\lambda=\mu$ and (c) $\lambda>\mu$ (k_p=0, H_x=0)

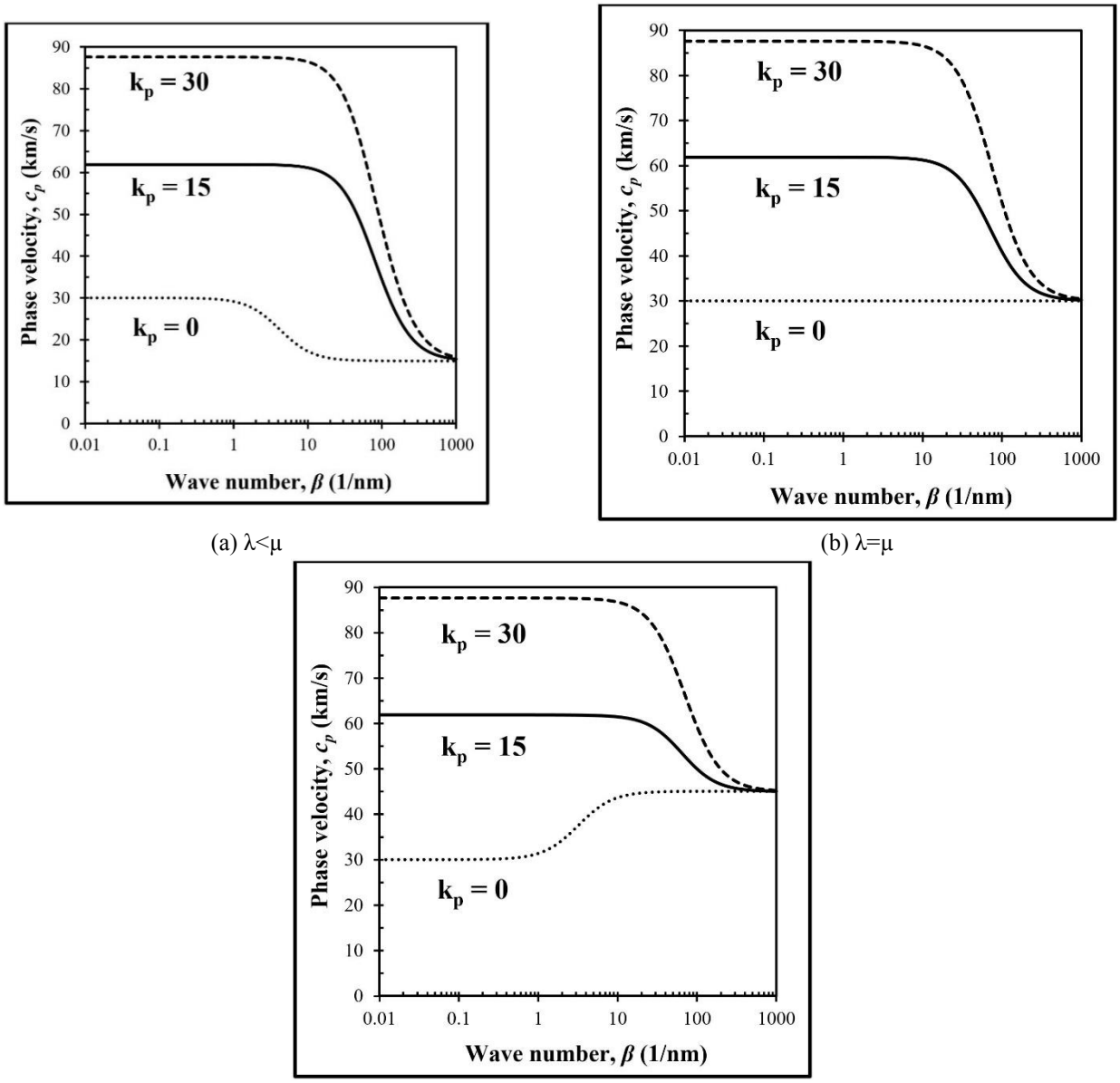

(a) λ<μ (b) λ=μ

(c) λ>μ

Fig. 5 Variation of phase velocity versus wave number for various values of Pasternak coefficient at (a) λ<μ, (b) λ=μ and (c) λ>μ (k_w=0, H_x=0)

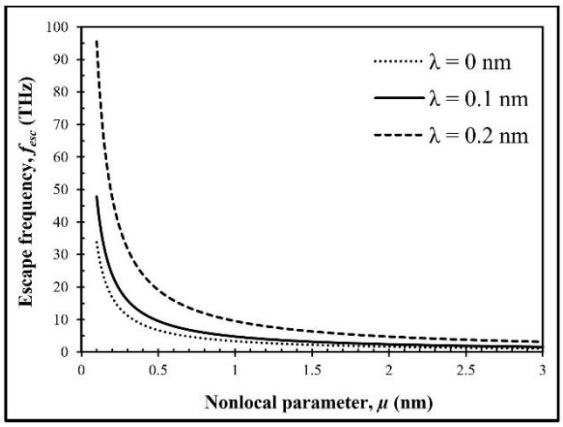

Fig. 6 Variation of escape frequency versus nonlocal parameter for various values of length scale parameter (k_w= k_p =0, H_x=0)

5. Conclusions

In this paper, wave propagation responses of SLGSs subjected to longitudinal magnetic field are studied in the framework of a refined two-variable plate theory incorporated with the NSGT. SLGS is considered to be rested on an elastic substrate including linear and nonlinear constants. The governing equations are derived applying a Hamiltonian approach with respect to the Lorentz force induced by the magnetic field. In the present part, a review is performed to highlight the most significant influences as follows:

- Wave dispersion responses of SLGSs can be amplified employing either lower nonlocal parameters or higher length scale parameters.
- Winkler parameter can generate an increase in the

value of phase velocity in a limited small range of wave numbers, roughly within $\beta = 0.04 \times 10^9$.

- As same as Winkler parameter, Pasternak coefficient has enough potential to intensify phase velocity values. However, effect of this parameter is not limited to small wave numbers and can be observed in high wave numbers too.
- Greater phase velocity amounts can be obtained once nonzero values are allotted to the magnetic field intensity compared to the condition in which this parameter is set to zero.
- Behavior of phase velocity is different in the cases of various length scale parameters. Phase velocity passes through a decreasing, constant and increasing path in high wave numbers when $\lambda<\mu$, $\lambda=\mu$ and $\lambda>\mu$, respectively.
- Escape frequency diminishes gradually as nonlocality increases. Also, higher escape frequencies can be achieved by utilizing greater length scale parameters.

References

Arash, B., Wang, Q. and Liew, K.M. (2012), "Wave propagation in graphene sheets with nonlocal elastic theory via finite element formulation", *Comput. Methods Appl. Mech. Eng.,* **223-224**, 1-9. https://doi.org/10.1016/j.cma.2012.02.002.

Aydogdu, M. (2009), "A general nonlocal beam theory: Its application to nanobeam bending, buckling and vibration", Physica E, **41**(9), 1651-1655. https://doi.org/10.1016/j.physe.2009.05.014.

Bellifa, H., Benrahou, K.H., Hadji, L., Houari, M.S.A. and Tounsi, A. (2016), "Bending and free vibration analysis of functionally graded plates using a simple shear deformation theory and the concept the neutral surface position", *J. Braz. Soc. Mech. Sci. Eng*., **38**, 265-275. https://doi.org/10.1007/s40430-015-0354-0.

Ebrahimi, F. and Barati, M.R. (2018), "Buckling analysis of nonlocal strain gradient axially functionally graded nanobeams resting on variable elastic medium", *Proceedings of the Institution of Mech. Eng., Part C: J. Mech. Eng. Sci.,* **232**(11), 2067-2078.

Ebrahimi, F., Barati, M.R. and Dabbagh, A. (2016a), "A nonlocal strain gradient theory for wave propagation analysis in temperature-dependent inhomogeneous nanoplates", *J. Eng. Sci.,***107**, 169-182. https://doi.org/10.1016/j.ijengsci.2016.07.008.

Ebrahimi, F., Barati, M.R. and Haghi, P. (2017), "Thermal effects on wave propagation characteristics of rotating strain gradient temperature-dependent functionally graded nanoscale beams", *J. Therm. Stresses,***40**(5), 535-547. https://doi.org/10.1080/01495739.2016.1230483.

Ebrahimi, F. and Salari, E. (2015), "A semi-analytical method for vibrational and buckling analysis of functionally graded nanobeams considering the physical neutral axis position", *CMES: Comput. Model. Eng. Sci*, **105**(2), 151-181.

Ebrahimi, F. and Barati, M.R. (2017), "Buckling analysis of piezoelectrically actuated smart nanoscale plates subjected to magnetic field", *J. Intelligent Mater. Syst. Struct.*, **28**(11), 1472-1490. https://doi.org/10.1177/1045389X16672569.

Ebrahimi, F. and Dabbagh, A. (2017c), "Nonlocal strain gradient based wave dispersion behavior of smart rotating magneto-electro-elastic nanoplates", *Mater. Res. Exp*., **4**(2), 025003. https://doi.org/10.1088/2053-1591/aa55b5.

Eltaher, M., Alshorbagy, A.E. and Mahmoud, F. (2013), "Vibration analysis of euler–bernoulli nanobeams by using finite element method", *Appl Math. Model.,* **37**(7), 4787-4797. https://doi.org/10.1016/j.apm.2012.10.016.

Eringen, A.C. (1972), "Linear theory of nonlocal elasticity and dispersion of plane waves", *J. Eng. Sci.,***10**(5), 425-435. https://doi.org/10.1016/0020-7225(72)90050-X.

Eringen, A.C. (1983), "On differential equations of nonlocal elasticity and solutions of screw dislocation and surface waves", *J. Appl. Phys.,***54**(9), 4703-4710. https://doi.org/10.1063/1.332803.

Farajpour, A., Yazdi, M.H., Rastgoo, A. and Mohammadi, M. (2016), "A higher-order nonlocal strain gradient plate model for buckling of orthotropic nanoplates in thermal environment", *Acta Mechanica,* **227**(7), 1849-1867. https://doi.org/10.1007/s00707-016-1605-6.

Fleck, N. and Hutchinson, J. (1993), "A phenomenological theory for strain gradient effects in plasticity", *J. Mech. Phys. Solids,***41**(12), 1825-1857. https://doi.org/10.1016/0022-5096(93)90072-N.

Arani, A.G., Haghparast, E. and Zarei, H.B. (2016), "Nonlocal vibration of axially moving graphene sheet resting on orthotropic visco-pasternak foundation under longitudinal magnetic field", *Physica B,* **495**, 35-49. https://doi.org/10.1016/j.physb.2016.04.039.

Arani, A.G. and M. Jalaei (2016), "Nonlocal dynamic response of embedded single-layered graphene sheet via analytical approach", *J. Eng. Math*., **98**(1), 129-144. https://doi.org/10.1007/s10665-015-9814-x.

Hadji, L. (2017a), "Analysis of functionally graded plates using a sinusoidal shear deformation theory", *Smart Struct. Syst.*, **19**(4), 441-448. https://doi.org/10.12989/sss.2017.19.4.441.

Hadji, L., Zouatnia, N. and Kassoul, A. (2017b), "Wave propagation in functionally graded beams using various higher-order shear deformation beams theories", *Struct. Eng. Mech.*, **62**(2), 143-149. https://doi.org/10.12989/sem.2017.62.2.143.

Hadji, L., Ait Amar Meziane, M., and Safa, A., (2018), "A new quasi-3D higher shear deformation theory for vibration of functionally graded carbon nanotube-reinforced composite beams resting on elastic foundation", *Struct. Eng. Mech.*, **66**(6), 771-781. https://doi.org/10.12989/sem.2018.66.6.771.

Khelifa, Z., Hadji, L., Hassaine Daouadji, T., and Bourada, M., (2018), "Buckling response with stretching effect of carbon nanotube-reinforced composite beams resting on elastic foundation", *Struct. Eng. Mech.*, **67**(2), 125-130. https://doi.org/10.12989/sem.2018.67.2.125.

Lam, D. Yang, C.F., Chong, A., Wang, J. and Tong, P. (2003), "Experiments and theory in strain gradient elasticity", *J. Mech. Phys. Solids,***51**(8), 1477-1508. https://doi.org/10.1016/S0022-5096(03)00053-X.

Lee, C., Wei, X., Kysar, J.W. and Hone, J. (2008), "Measurement of the elastic properties and intrinsic strength of monolayer graphene", *Science,* **321**(5887), 385-388. https://doi.org/10.1126/science.1157996

Li, L. and Hu, Y. (2015), "Buckling analysis of size-dependent nonlinear beams based on a nonlocal strain gradient theory", *J. Eng. Sci.,***97**, 84-94.

Lim, C., Zhang, G. and Reddy, J. (2015), "A higher-order nonlocal elasticity and strain gradient theory and its applications in wave propagation", *J. Mech. Phys. Solids,***78**, 298-313.

Liu, H. and Yang, J.L. (2012), "Elastic wave propagation in a single-layered graphene sheet on two-parameter elastic foundation via nonlocal elasticity", *Physica E,* **44**(7), 1236-1240. https://doi.org/10.1016/j.physe.2012.01.018.

Malekzadeh, P., Setoodeh, A. and Beni, A. A. (2011), "Small scale effect on the free vibration of orthotropic arbitrary straight-sided quadrilateral nanoplates", *Composite Structures,* **93**(7), 1631-1639. https://doi.org/10.1016/j.compstruct.2011.01.008.

Murmu, T., McCarthy, M.A. and Adhikari, S. (2013), "In-plane magnetic field affected transverse vibration of embedded single-layer graphene sheets using equivalent nonlocal elasticity approach", *Compos. Struct.,* **96**, 57-63.

https://doi.org/10.1016/j.compstruct.2012.09.005.
Murmu, T. and Pradhan, S. (2009), "Vibration analysis of nano-single-layered graphene sheets embedded in elastic medium based on nonlocal elasticity theory", *J. Appl. Phys.,* **105**(6), https://doi.org/10.1063/1.3091292.
Narendar S. and Gopalakrishnan, S. (2012a), "Study of terahertz wave propagation properties in nanoplates with surface and small-scale effects", *J. Mech. Sci.,* **64**(1), 221-231. https://doi.org/10.1016/j.ijmecsci.2012.06.012.
Narendar S. and Gopalakrishnan, S. (2012b), "Temperature effects on wave propagation in nanoplates", *Composites Part B,* **43**(3), 1275-1281. https://doi.org/10.1016/j.compositesb.2011.11.029.
Natarajan S., Chakraborty, S., Thangavel, M., Bordas, S. and Rabczuk, T. (2012), "Size-dependent free flexural vibration behavior of functionally graded nanoplates", *Comput. Mater. Sci.,***65**, 74-80. https://doi.org/10.1016/j.commatsci.2012.06.031.
Larbi, L.O., Hadji, L., Meziane, M. A.A. and Adda Bedia, E.A. (2018), "An analytical solution for free vibration of functionally graded beam using a simple first-order shear deformation theory", *Wind Struct.*, **27**(4), 247-254. https://doi.org/10.12989/was.2018.27.4.247.
Pradhan S. and T. Murmu (2010), "Small scale effect on the buckling analysis of single-layered graphene sheet embedded in an elastic medium based on nonlocal plate theory", *Physica E,***42**(5), 1293-1301. https://doi.org/10.1016/j.physe.2009.10.053.
Pradhan, S.C. and Kumar, A. (2011), "Vibration analysis of orthotropic graphene sheets using nonlocal elasticity theory and differential quadrature method", *Compos. Struct.,* **93**(2), 774-779. https://doi.org/10.1016/j.compstruct.2010.08.004.
Rouhi S. and Ansari, R. (2012), "Atomistic finite element model for axial buckling and vibration analysis of single-layered graphene sheets", *Physica E,* **44**(4), 764-772. https://doi.org/10.1016/j.physe.2011.11.020.
Seol J.H., Jo, I., Moore, A.L., Lindsay, L., Aitken, Z., Pettes, M., Li, X., Yao, Z., Huang, R., Broido, D., Mingo, N., Ruoff, R. and Shi, L. (2010), "Two-dimensional phonon transport in supported graphene", *Science,* **328**(5975), 213-216. https://doi.org/10.1126/science.1184014.
Wang, Q. and Varadan, V. (2007), "Application of nonlocal elastic shell theory in wave propagation analysis of carbon nanotubes", *Smart Mater. Struct.,***16**(1), 178. https://doi.org/10.1088/0964-1726/16/1/022.
Wang, Y.Z., Li, F.M. and Kishimoto, K. (2010), "Scale effects on the longitudinal wave propagation in nanoplates", *Physica E*,**42**(5),1356-1360. ttps://doi.org/10.1016/j.physe.2009.11.036.
Xiao, W., Li, L. and Wang, M. (2017), "Propagation of in-plane wave in viscoelastic monolayer graphene via nonlocal strain gradient theory", *Appl. Phys. A,***123**(6), 388. https://doi.org/10.1007/s00339-017-1007-1.
Zouatnia, N., Hadji, L. and Kassoul, A. (2017), "An analytical solution for bending and vibration responses of functionally graded beams with porosities", *Wind Struct.*, **25**(4), 329-342. https://doi.org/10.12989/was.2017.25.4.329.
Zenkour, A.M. (2016), "Nonlocal transient thermal analysis of a single-layered graphene sheet embedded in viscoelastic medium", *Physica E,* **79**, 87-97. https://doi.org/10.1016/j.physe.2015.12.003.